Desalination and Water Treatment
www.deswater.com

doi: 10.5004/dwt.2018.22881

128 (2018) 330–340
October

The analysis of possibilities to increase the efficiency of the zero-emission combined cycle power plant with the membrane reactor

Marcin Job, Janusz Kotowicz*

Institute of Power Engineering and Turbomachinery, Silesian University of Technology, Konarskiego 18, 44-100 Gliwice, Poland, Tel. +48 32 2371745; email: janusz.kotowicz@polsl.pl

Received 27 May 2018; Accepted 17 July 2018

ABSTRACT

Oxy-combustion is one of the promising carbon capture technologies in fossil fuel power plants. Currently, the greatest challenge is to find ways to reduce the energy consumption of the process of oxygen separation from the air. The use of oxygen ion transport membranes (ITM), intensively developed in recent years, especially in terms of use in zero-emission energy units, may be a solution of this problem. Due to high ITM operating temperatures, they are thermally integrated with a gas turbine, placed within the structure of a membrane reactor, which replaces the combustor in the gas turbine installation, performing three functions: separation of oxygen from the air in the ITM, heating the oxygen-depleted air and fuel combustion. The paper presents a model of the zero-emission combined cycle power plant with the membrane reactor and results of thermodynamic analysis for the basic model with assumptions corresponding to currently available technologies and membrane materials. The analyzes of the influence of the most important membrane parameters, taking into account the possibilities of improving materials used for ITM as a result of technological progress, on the parameters of AZEP plant are made. The basic model of the analyzed power plant obtained the electricity generation efficiency of 51.2%, which is a competitive result compared with other units equipped with carbon capture. However, the analysis for improved ITM materials showed that at the case of assumed technological progress it is possible to increase net electric efficiency of AZEP plant by 0.5%–0.8% point, achieving up to almost 52%. The higher efficiency was achieved for the lower compression ratio of gas turbine than for the basic model, which could also lead to lower capital costs. Therefore, the presented results confirmed that the further development of the ITM for the power plants with membrane reactors would contribute to both higher efficiency of electricity production and lower investment costs of these power plants.

Keywords: Oxy-combustion; Membrane reactor; Ion transport membrane ITM; Zero-emission combined cycle power plant; AZEP

1. Introduction

Dynamic changes made over last years in energy policies of many countries, in particular in the European Union, are aimed at counteracting the climate changes by reducing greenhouse gas emissions, including primarily carbon dioxide. This implies new, unprecedented challenges for fossil fuel-fired power plants, currently playing a dominant role in the energy sector [1,2]. In the face of the growing share of renewable energy sources, often characterized by a large irregularity of electricity production overtime, a particularly important aspect is to ensure the security of energy supply and to significantly reduce greenhouse gas emissions at the same time. As one of the key activities, the introduction of zero-emission electricity production from fossil fuels is proposed, which can be implemented through the implementation of carbon capture and storage (CCS) installations. Three main technologies for CO_2 separation can be distinguished: postcombustion, precombustion, and oxy-combustion. Furthermore,

* Corresponding author.

Presented at the XII Scientific Conference "Membranes and Membrane Processes in Environmental Protection" – MEMPEP 2018 13–16 June 2018, Zakopane, Poland

within CCS installation, the separated gas must be prepared and directed to the storage place. The preparation involves the need to clean, dry, and compress the captured gas. Regardless of the CO_2 capture method, the introduction of such an installation is associated with a decrease in the efficiency of electricity production and a significant increase in the capital costs of such power plants, due to the presence of additional elements and the increased complexity of the technological process [3–5].

1.1. Oxy-combustion technology

The air, consisting of approximately 79% N_2 and 21% O_2, is used as an oxidant in conventional combustion process. In this case, depending on used fuel, the flue gas consists mostly of N_2, O_2, H_2O, and only a few percent of CO_2. The separation of CO_2 from the flue gas with such a low concentration of this gas is a highly energy-intensive process. In turn, the oxy-combustion technology is based on the combustion of a fuel in the oxidant atmosphere with reduced nitrogen content. The oxidant, obtained by the air separation, consists almost exclusively of O_2 and only up to several percent of N_2. As a result, nitrogen is almost eliminated from the combustion process, while oxygen, most often diluted with CO_2 and/or H_2O, reacts with the fuel with the lowest possible excess oxidant ratio. The flue gas consists almost exclusively of CO_2, H_2O, and small amounts of other gases depending on the oxygen separation technology and the type and composition of the fuel used. The obtained gas may only require an additional purification in order to meet the requirements for the gas intended for utilization or storage [6,7].

Power plants powered by natural gas, consisting mainly of hydrocarbons and containing minimal amounts of pollutants, are predisposed for the application of oxy-combustion technology. Therefore, natural gas power plants with oxy-combustion technology the separation of CO_2 do not require additional gas cleaning process, while the gas processing itself is limited to the flue gas cooling and condensation of water vapor. Moreover, since 100% of the produced CO_2 is captured along with any remaining gaseous impurities, the oxy-combustion technology is the only one that may be called fully zero-emission in terms of gaseous pollutions. The only products discharged to the atmosphere are the air with reduced oxygen content, water, and dissipated heat.

The biggest challenge for the power units with oxy-combustion is the need to separate large amounts of oxygen from the air. The air separation unit (ASU) is an autonomous system here. At present, the technical possibilities of oxygen production with the required quantity and purity at the level of 95.0%–99.5% are only revealed by cryogenic ASU, which is mature, but high energy-consuming technology [8–10]. Other oxygen separation techniques are also developed, among others adsorption methods, low-temperature and high-temperature membranes or hybrid systems. These methods still do not allow for the production of oxygen of the required quantity and quality, but they show that in the future a reduction in energy consumption associated with the separation of oxygen from the air may be expected [11–15].

2. Ion transport membranes

The ion transport membranes (ITM) have been known for many years, while in recent decades they were intensively developed, especially in terms of use in zero-emission energy units. They are made of ceramic materials, which heated to a sufficiently high temperature of at least approximately 700°C, allow for the passage of oxygen ions through their structure. There are mainly perovskite or fluorite membranes having in their structure vacancies accepting oxygen ions, which can permeate through the membrane passing between these vacancies. On the other hand, the dense structure of ceramic membranes is impermeable to other gases. This structure of ITM makes that, assuming no leaks, cracks or other defects in the construction of the membrane, they can be used to produce pure oxygen [6,16–18].

The oxygen separation process through the membrane consists of numerous phenomena occurring in the membrane, with each of these phenomena can have an impact on the total oxygen flux permeating through the membrane. However, in membrane models made for the purpose of energy system analyzes, the influence of most of these phenomena may be neglected, as they may affect the separation process only under certain conditions [19]. Two processes are crucial in this case. For large membrane thickness, the oxygen diffusion is limited by the volumetric diffusion of oxygen through the membrane, depending on the difference in oxygen chemical potentials. In turn, for thin membranes, below the characteristic thickness of the membrane, the greater limitation is the surface transfer of oxygen, in which the driving force is the difference in oxygen partial pressures [20]. This feature means that reducing the thickness of the membrane much below the characteristic thickness does not correspond to a significant increase in the flow of oxygen permeated through the membrane. For a membrane thickness greater than the characteristic thickness, the Nernst–Einstein relationship is valid and the oxygen flow is inversely proportional to the membrane thickness:

$$j_{O_2} = \frac{\sigma_i \times RT_M}{4d(nF)^2} \times \ln\left(\frac{\left(p_{O_2}\right)_A}{\left(p_{O_2}\right)_G}\right) \tag{1}$$

where j_{O_2} – the unit flow of oxygen ions permeated through the membrane, mol/(m^2 s); σ_i – ion conductivity of the material, S/m; R – universal gas constant, $R \approx 8.3145$ J/(mol K); T_M – membrane temperature, K; d – membrane thickness, m; n – number of carrier charges (for oxygen ions $n = 2$); F – Faraday constant, $F \approx 9.6485 \times 10^4$ C/mol; $\left(p_{O_2}\right)_A$ – partial oxygen pressure on the air side of membrane, kPa; and $\left(p_{O_2}\right)_G$ – partial oxygen pressure on the sweep gas side of membrane, kPa.

For many membranes the characteristic thickness is below 100 μm, but such thin membranes are reinforced by a porous support made of the same or similar material as the dense layer. The membrane itself can withstand constant operation in temperatures of up to 1,100°C, which are too high for a porous support, for which the use of temperatures close to 1,000°C causes sintering, which reduces its porosity and, thus, the performance of such a membrane [16]. At the

current stage of the development, small size membranes are produced and tested in many research centers around the world. The literature particularly distinguishes membranes from BSCFO perovskite material ($Ba_{0,5}Sr_{0,5}Co_{0,8}Fe_{0,2}O_{2-d}$), which achieves high values of oxygen ion conductivity compared with other materials [21–24]. Authors in this article also adopted the membrane operating parameters characteristic for this material. Among the key issues to be mastered prior to the commercialization of ITMs, there is an improvement of their efficiency, chemical and thermal stability, mechanical strength and a reduction of the materials prices [16].

3. Oxy-combustion power plants with ion transport membranes

ITM may be used to build an external ASU, but high temperatures of operation allow for their integration with the gas turbine cycle, therefore the concepts of power plants using ITMs are considered as a separate group of power plant with oxy-combustion solutions. This solution allows to reduce the power plants efficiency drop associated with the production of oxygen [6]. So far, no pilot power plant using ITMs has been created. At the current development state, research aimed at confirming the legitimacy of implementing this technology on a commercial scale is conducted. In addition to issues related to the development of ITMs themselves, the literature contains a number of concepts of zero-emission power plants integrated with ITM, among which the most frequently mentioned are AZEP (advanced zero emission power) [25] and ZEITMOP (zero emission ITM oxygen power) [6]. In AZEP plants, instead of the combustion chamber of the gas turbine, the use of a membrane reactor is proposed, which performs three basic functions: (I) separation of oxygen from compressed air through the ITM; (II) heat exchange to heat the oxygen-depleted air; (III) near-stoichiometric combustion of gaseous fuel. The flue gas in the semiopen membrane reactor cycle is composed almost exclusively of CO_2 and H_2O, so the CO_2 capture from the flue gas stream leaving the membrane reactor is limited to the removal of the excess moisture. The flue gas leaving the membrane reactor cycle has a high temperature, therefore, before CO_2 capture, its heat energy is utilized. Two solutions of the AZEP plant differed in the manner of the flue gas heat utilization can be specified in the literature. In the first concept, the flue gas is directed to the heat recovery steam generator (HRSG), allowing to increase the steam turbine power [25,26]. In the second concept, the increased pressure in the membrane reactor cycle is used and the flue gas leaving this cycle is expanded in a gas-steam (CO_2/H_2O) turbine [27,28]. The efficiency of electricity generation exceeding 50% is indicated for both solutions, and the efficiency drop associated with the use of CO_2 capture is estimated at about 5% points.

The studies on modeling and analyzes of AZEP plants available in the literature indicate on the need for multicriteria analyzes of power plants integrated with ITM, which will allow to estimate the potential of this solution and to identify its key aspects requiring significant improvement before commercialization [29,30]. The paper presents the results of thermodynamic analyzes of combined cycle power plant integrated with a membrane reactor with an increased gas pressure and a gas-steam turbine. The membrane reactor numerical model made by authors allows for the initial calculation of the key parameters of the ITM and a membrane reactor, necessary to determine the thermodynamic efficiency of the AZEP plant, without the need to determine the geometric parameters of the membrane and heat exchangers. The impact of the improvement of the most important ITM parameters on the power plants efficiency and membrane reactor surface areas was also assessed. It allowed to estimate the potential of using ITM in AZEP plants in the case of developing new membranes with more favorable properties or their improvement within currently known materials used for their production. Thus, the presented analyzes showed which of the ITM properties constituted to the greatest constraints and how big impact on the AZEP plant operation could bring their improvement.

4. The model of the power plant with a membrane reactor

The analyzed zero-emission combined cycle power plant with a membrane reactor is based on the AZEP cycle concept [25], therefore, it is marked with this symbol in this paper. The structure of the power plant model is shown in Fig. 1.

The developed AZEP plant model consists of a gas turbine GT integrated with a membrane reactor MR, a steam cycle with HRSG SC and a carbon dioxide conditioning unit CCU. Models of discussed AZEP plant components were made and integrated using GateCycle™ software [31] and own calculation codes with the use of Microsoft Excel environment.

4.1. Gas turbine and steam cycle

In the AZEP plant model assumed the constant electrical gas turbine power N_{elGT}, obtained at the generator terminals, equal to 200 MW. The gas turbine was supplied with air of parameters 15°C, 101.325 kPa and relative humidity of 60%. The air filter pressure loss was 1%. The compressor pressure ratio (defined as the ratio of outlet pressure to inlet pressure) was equal to $\beta = 20$. The compressed air was directed to the membrane reactor, where it passed over part of the oxygen and was heated to a temperature of t_{3a} = 1,280°C, and then was expanded in the turbine to a pressure of p_{4a} = 105.5 kPa. The isentropic efficiencies of the compressor and the turbine were, respectively, $\eta_{iC} = 0.88$ and $\eta_{iT} = 0.90$, mechanical efficiencies were equal to $\eta_{mC} = \eta_{mT} = 0.995$. The open-air cooling of expander blades was used in the gas turbine. The air flow drawn from behind the compressor for cooling was determined based on the equation of heat flow in the turbine blade system, shown, for example, in Refs. [32,33].

The oxygen-depleted air leaving the gas turbine, with the temperature t_{4a} = 539°C, for the above-mentioned assumptions, was directed to the HRSG in the steam cycle. The steam cycle was based on the operation of a steam turbine ST consisting of three sections: high pressure (*h*), intermediate pressure (*i*), and low pressure (*l*). The steam turbine was powered by steam generated in a triple-pressure HRSG with steam reheating before the intermediate pressure steam turbine section. The temperature and pressure of live steam and reheated steam were, respectively, 519°C/18.0 MPa and 519°C/4.0 MPa. The applied steam temperature resulted

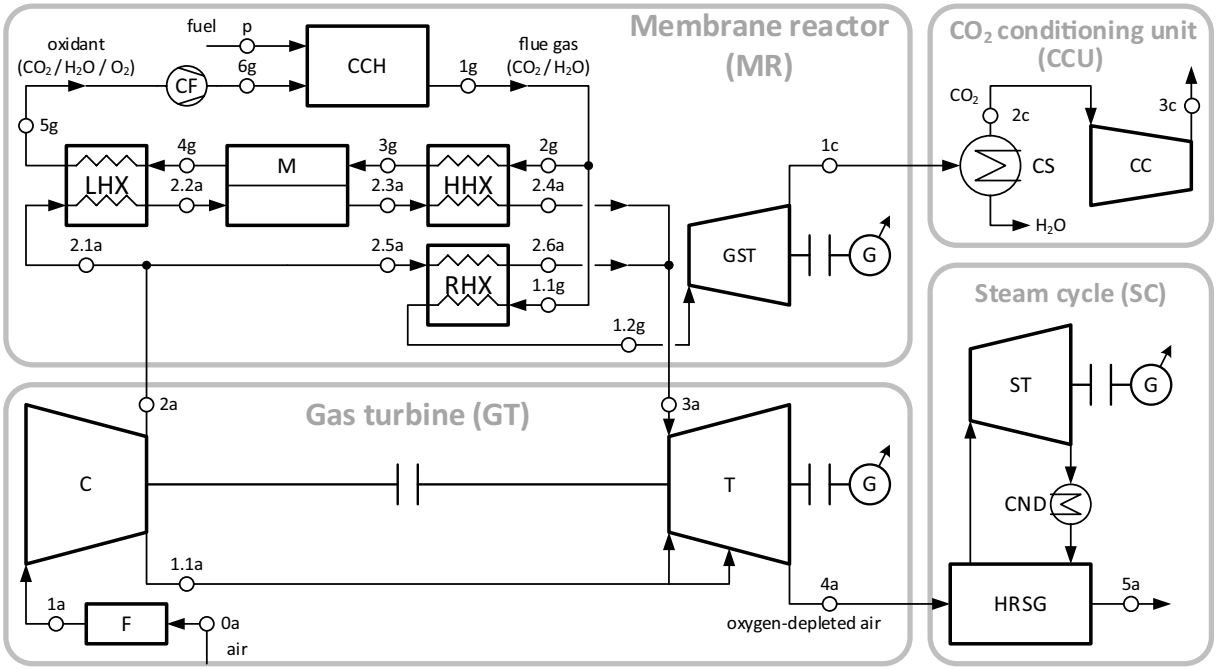

Fig. 1. The structure of the combined cycle power plant with membrane reactor AZEP (C – compressor, CC – CO_2 compressor, CCH – combustion chamber, CF – circulation fan, CND – condenser, CS – condensation separator, F – filter, G – generator, GST – gas-steam turbine HRSG – heat recovery steam generator, LHX, HHX, RHX – heat exchangers, M – ion transport membrane, ST – steam turbine, and T – turbine).

from the temperature difference at the HRSG hot end, equal to 20 K. The pressure of the low-pressure steam is 0.3 MPa. The steam turbine isentropic efficiency was assumed at the level of $\eta_{i.TP}$ = 0.90. The condenser pressure was equal to 5 kPa. Pressure losses in the steam cycle were: in economizers 1%, in evaporators 4%, in steam superheaters 3%, before the high-pressure steam turbine section 3%, and before other steam turbine sections 2%. Such design parameters of the steam cycle as steam pressure levels and temperature differences in HRSG were selected by means of optimization with the use of a genetic algorithm, which was successfully used in similar optimization problems [34].

The efficiency of all generators used in the AZEP plant was η_G = 0.985. The total own needs rate of machinery and auxiliary equipment in GT and SC installations was assumed to be equal to 2% of the gross electric power of the power plant $N_{el.gross}$.

4.2. Membrane reactor and carbon conditioning unit

In the membrane reactor model, assumptions corresponding to the current technological and material limitations of the used components, was applied. The most important membrane material properties used in the model were assumed based on data for BSCFO [20,22]. The air temperature at the membrane cold end corresponded to its minimum operating temperature and was equal to $t_{2.2a} = (t_M)_{min}$ = 700°C, while the flue gas temperature at the membrane hot end corresponded to the maximum operating temperature, which, limited by the use of a porous carrier, was equal to $t_{3g} = (t_M)_{max}$ = 900°C. Due to the narrow temperature range of the ITM operation, the membrane modules with additional heat exchangers were used in the membrane reactor. The low-temperature heat exchanger LHX before the membrane was responsible for heating the compressed air to the required temperature $t_{2.2a}$, while the high-temperature heat exchanger HHX behind the membrane was intended to heat the air to the temperature significantly above its upper operating temperature. Membrane modules with chessboard structure allowed to achieve the density of heat exchange surfaces at the level of 800 – 1,000 m^2/m^3, therefore the use of surface areas of the order of hundreds of thousands of square meters is possible in big power plants [25].

Currently, the maximum operating temperature of heat exchangers is about 1,300°C [25], therefore, a flue gas temperature of t_{2g} = 1,300°C was assumed at the hot end of HHX. With an assumption of a constant temperature difference at the hot end of HHX, equal to $\Delta T_{HE.HHX}$ = 20 K, the oxygen-depleted air temperature at the HHX hot end was $t_{2.4a} = t_{3a}$ = 1,280°C. Basing on the known air temperature in LHX (cold end temperature dependent on the compression ratio, equal to $t_{2.1a} = t_{2a}$, hot end temperature was $t_{2.2a}$ = 700°C) and the flue gas temperature at the LHX hot end (t_{4g}), which was determined in the membrane calculation model, the LHX cold end flue gas temperature (t_{5g}) was calculated. Part of the compressed air directed to the membrane reactor was heated in the regenerative heat exchanger RHX by the flue gas stream leaving the membrane reactor. Temperature at the RHX hot end corresponded to HHX ($t_{1.1g} = t_{2g}$, $t_{2.6a} = t_{2.4a}$), and the air temperature at the RHX cold end was the same as in

LHX ($t_{2.5a} = t_{2.1a}$). The LHX cold end temperature difference was assumed to be equal to $\Delta T_{CE.RHX}$ = 40 K. The heat losses in LHX, HHX, and RHX were 0.5%. Areas of heat exchangers were determined in accordance with the equation:

$$\dot{Q} = k \times A \times \Delta T_M \tag{2}$$

where $\dot{Q}$ – heat flux, W; A – surface area, m²; k – heat transfer coefficient of heat exchanger, W/(m² K); and ΔT_M – mean logarithmic temperature difference at both sides of heat exchanger, K.

Based on [20], heat transfer coefficients k were adopted, respectively, for LHX, HHX, and RHX heat exchangers: k_{LHX} = 70 W/m² K, k_{HHX} = 100 W/m²·K, and k_{RHX} = 90 W/m²·K. The total heat exchange surface in a membrane reactor was a sum of the surfaces of all heat exchangers and the membrane:

$$A_{RM} = A_{LHX} + A_M + A_{HHX} + A_{RHX} \tag{3}$$

The total pressure losses in the membrane modules are indicated in the literature at the level of 12%–14% [20,35]. In the developed model, the total air and flue gas pressure losses coefficients (defined as the difference between inlet and outlet pressure divided by the inlet pressure) in the membrane module were assumed to be equal to $\zeta_A = \zeta_G$ = 0.125. Following the analyzes presented in Ref. [20], assumed distribution of total pressure losses was as follows: 60% at the inlet manifold, 20% at the outlet collector, whereas the channels of the membrane modules were responsible for remaining 20%. A linear pressure drop in channels of the membrane modules, proportional to the surface of the module, was assumed.

The issue of modeling of the ITM involves simultaneous processes of mass and heat exchange on the membrane surface in the presence of pressure losses. No heat losses in the membrane were assumed in the model. It was necessary to determine the membrane surface A_M and the heat flow transferred through the membrane surface. The membrane model used the Nernst–Einstein relationship (Eq. (1)), taking into account the membrane surface and the membrane temperature change resulting from the heat exchange:

$$\dot{m}_{O_2} = A_M \times M_{O_2} \times \int_0^{A_M} \left\{ \frac{\sigma_i \times RT_M}{4d\left(nF\right)^2} \times \left(\frac{\left(p_{O_2}\right)_A}{\left(p_{O_2}\right)_G} \right) \right\} dA_M \tag{4}$$

where A_M – membrane surface, m²; M_{O_2} – specific molar mass of oxygen, kg/kmol; and A constant factor C_1 was distinguished from Eq. (4), defined by the dependence:

$$C_1 = \frac{R}{4d\left(nF\right)^2} \tag{5}$$

Ion conductivity σ_i is a characteristic parameter of the membrane material. The σ_i values are subjected to the Arrhenius temperature dependence, according to the equation:

$$\sigma_i \times T_M = C_2 \times e^{-\frac{E_a}{R \times T_M}} \tag{6}$$

where E_a – activation energy for ion conductivity (in the model E_a = 56 kJ/mol); and C_2 – constant coefficient characteristic for the membrane (in the model C_2 = 517,236.2).

The value of C_2 coefficient was determined by fitting Eq. (6), using the least squares method, to the values of σ_i determined experimentally for BSCFO, taken from Ref. [22]. A membrane structure with a porous support with the thickness of dense layer equal to d = 0.1 mm was assumed. In order to determine the membrane surface A_M and its other operating parameters, a simplified model was used, in which the membrane was divided into n (n = 100) serially connected parts. In each part of the membrane, constant pressure and temperature of gases, being arithmetic means of inlet and outlet values; temperature of a given membrane segment equal to arithmetic mean temperature of the gases on both sides of the membrane; and linear change in molar oxygen proportion with the membrane surface, were assumed. The membrane model assumed equal flow of oxygen permeated through the surface of each membrane part:

$$\left(\dot{m}_{O_2}\right)_i = \frac{1}{n} \times \dot{m}_{O_2} \tag{7}$$

The total oxygen flow permeated through the membrane was described by the oxygen recovery ratio from the air R_a:

$$R_a = \frac{\dot{m}_{O_2}}{\left(\dot{m}_{O_2}\right)_{2.2a}} \tag{8}$$

where $\left(\dot{m}_{O_2}\right)_{2.2a}$ is mass oxygen flow rate in the air at the membrane inlet.

In the model, for given values of R_a and streams of gases on both sides of the membrane, a surface of each membrane part $A_{M.i}$ required to permeate assumed flux of oxygen $\left(\dot{m}_{O_2}\right)_i$ $\left(\dot{m}_{O_2}\right)_i$ was calculated using the Eqs. (4)–(7). In the next step, for calculated surface $A_{M.i}$, a heat transfer through each membrane part $\dot{Q}_{M.i}$ was determined according to dependence Eq. (2), for the membrane heat transfer coefficient k_M = 90 W/m²K. A flue gas ratio coefficient γ_G, which is a ratio of membrane inlet flue gas flow (at the hot end) to the membrane inlet airflow (at the cold end), defined by Eq. (9), was responsible for the regulation of the flue gas cycle in the membrane reactor.

$$\gamma_G = \frac{\dot{m}_{3g}}{\dot{m}_{2.2a}} \tag{9}$$

This ratio has a crucial influence on the temperature differences in the membrane modules and was regulated so as to reach the assumed oxygen-depleted air temperature at the hot end of HHX ($t_{2.4a}$ = 1,280°C).

The flue gas with oxidant leaving the membrane module was directed to the combustion chamber CCH through the circulating fan CF. The flue gas pressure and temperature at the combustion chamber outlet were equal to p_{1g} = 1,800 kPa and t_{1g} = 1,300°C. Methane (100% CH_4) with parameters of 15°C, 3,500 kPa and lower heating value LHV = 50.049 MJ/kg were used as a fuel. The combustion chamber efficiency was

η_{KS} = 0.99, while the pressure losses in the combustion chamber were 4%. Considering the CO_2 capture, excess oxygen in the flue gas is undesired, therefore, near-stoichiometric combustion was maintained with a slight excess of oxygen to maintain stability of the combustion process. For this purpose, the oxygen recovery ratio in membrane R_a (Eq. (8)) was regulated so as to maintain a constant oxygen content in combustion chamber outlet flue gas at the level of $(O_2)_{1g}$ = 2%. Due to the mutual dependence of the membrane surface, temperatures and pressure losses of the gases, both calculations, for the membrane and for the entire membrane reactor cycle were performed iteratively, matching the two main regulation parameters of γ_G and R_a in subsequent iterations. The computational algorithms of the ITM and the membrane reactor cycle are described in detail in Ref. [36].

The flue gas stream leaving the membrane reactor cycle, after cooling in RHX, was expanded in the gas-steam turbine GST to a pressure of p_{1c} = 105.5 kPa and then directed to the carbon conditioning unit CCU. A simple design of the gas-steam turbine, with no blade cooling system and isentropic efficiency equal to η_{iGST} = 0.85, was assumed. The circulation fan isentropic efficiency was assumed at the level of η_{iCF} = 0.80. The auxiliary power of the membrane reactor ΔN_{MR} was equal to the electric power consumed by the circulating fan N_{elCF} reduced by the electric power generated by the gas-steam turbine N_{elGST}, according to the dependence:

$$\Delta N_{MR} = N_{elCF} - N_{elGST} \tag{10}$$

The flue gas directed to CCU consisted almost exclusively of CO_2, H_2O, and a small amount of O_2, therefore, the required CO_2 purity, adopted at the level of 90% mol., was achieved by removing the excess moisture, without the need for any additional purification of the captured gas. The gas was cooled to the temperature of 30°C and dried in condensation separator CS. Then, an eight-section compression process of captured CO_2 was performed. In first seven sections of the CO_2 compression CC, the gas was compressed to the pressure of 6.5 MPa, with identical compression ratios in each section and intercooling to the temperature of 30°C. In the last section the gas was cooled to the temperature of 15°C and condensed under subcritical conditions. This allowed for the use of liquid CO_2 pump, compressing the gas to the pressure of 13 MPa. The isentropic efficiency of compressors and CO_2 pump was equal to 80%. Waste heat from intercoolers was dispersed to the environment.

5. Thermodynamic analysis

The most important indicator determining the efficiency of operation of power plants, including the analyzed AZEP plant, is the efficiency of electricity generation. The gross electric efficiency $\eta_{el.gross}$ is expressed by the dependence:

$$\eta_{el.gross} = \frac{N_{el.gross}}{\dot{m}_f \mathrm{LHV}} = \frac{N_{elGT} + N_{elST}}{\dot{m}_f \mathrm{LHV}} \tag{11}$$

where $N_{el.gross}$ – gross electric power of combined cycle power plant, MW; N_{elGT} – gas turbine electric power, MW; N_{elST} – steam turbine electric power, MW; and $\dot{m}_f$LHV – fuel chemical energy flux, MW.

Electric efficiency of gas turbine η_{elGT} and steam cycle η_{elSC} is described by relations:

$$\eta_{elGT} = \frac{N_{elGT}}{\dot{m}_f \mathrm{LHV}} \tag{12}$$

$$\eta_{elSC} = \frac{N_{elSC}}{\dot{Q}_{4a}} \tag{13}$$

where $\dot{Q}_{4a}$ is a heat flow rate of oxygen-depleted air feeding the HRSG.

The net electric efficiency of AZEP plant is defined by analogy to Eq. (11), but it applies to the net electric power of AZEP plant N_{el}, taking into account the total own needs of the power plant ΔN_{el}:

$$\eta_{el} = \frac{N_{el}}{\dot{m}_f \mathrm{LHV}} = \frac{N_{el.gross} - \Delta N_{el}}{\dot{m}_f \mathrm{LHV}} \tag{14}$$

$$\Delta N_{el} = \sum \Delta N_i = \Delta N_{CC} + \Delta N_{CCU} + \Delta N_{MR} \tag{15}$$

where ΔN_{CC} – auxiliary power of gas turbine and steam cycle installations, ΔN_{CCU} – auxiliary power of carbon conditioning unit, and ΔN_{MR} – auxiliary power of membrane reactor (Eq. (10)).

The total own needs ratio of AZEP plant is described by dependence:

$$\delta_{el} = \frac{\Delta N_{el}}{N_{el.gross}} \tag{16}$$

Among the AZEP plant operation parameters presented in Chapter 4, the following were obtained as a result of an optimization of: gas turbine pressure ratio (β = 20), oxygen-depleted air temperature at the turbine inlet (t_{3a} = 1,280°C), flue gas pressure in membrane reactor (p_{1g} = 1,800°C), air temperature at the membrane cold end ($t_{2.2a}$ = 700°C), and flue gas temperature at the gas-steam turbine inlet ($t_{1.2g}$ = 482°C). A boundary condition in the selection of optimum values of abovementioned parameters was the maximum heat exchange surface in the membrane reactor, equal to $(A_{MR})_{max}$ = 200,000 m^2. Multistage analyzes and the selection of optimal AZEP plant operating parameters are presented by authors in detail in Ref. [37]. The most important operation parameters of AZEP plant are presented in Table 1.

The gas turbine in the AZEP plant model achieved the electric efficiency η_{elGT} at the level of 35%, which was a low value compared with the current high-power gas turbines with efficiency exceeding 40%. Among the factors responsible for low efficiency one could distinguished:

- Low temperature of the oxygen-depleted air supplied to the turbine (t_{3a} = 1,280°C), resulting from limited endurance of the materials used in heat exchangers.

Table 1
Selected characteristic parameters of AZEP plant model

Parameter	Symbol, unit	Value
Fuel chemical energy flux	$\dot{m}_f LHV$, MW	571.0
Gas turbine electric power	N_{elGT}, MW	200.0
Turbine internal power	N_{iT}, MW	497.6
Compressor internal power	N_{iC}, MW	290.6
Gas turbine electric efficiency	η_{elGT}, –	0.3502
Gas turbine outlet air heat flow	$\dot{Q}_{4a}$, MW	336.1
Steam turbine electric power	N_{elST}, MW	106.4
Steam cycle electric efficiency	η_{elSC}, –	0.3144
Power plant gross electric power	$N_{el.gross}$, MW	306.4
Power plant gross electric efficiency	$\eta_{el.gross}$, –	0.5366
Gas turbine and steam cycle own needs	ΔN_{CC}, MW	6.1
Gas-steam turbine electric power	N_{elGST}, MW	23.6
Circulation fan electric power	N_{elCF}, MW	20.0
Membrane reactor own needs	ΔN_{MR}, MW	–3.6
CO_2 conditioning unit own needs	ΔN_{CCU}, MW	11.4
Total power plant own needs	ΔN_{el}, MW	13.9
Total power plant own needs ratio	δ_{el}, –	0.0454
Power plant net electric power	N_{el}, MW	292.5
Power plant net electrical efficiency	η_{el}, –	0.5122
Oxygen recovery ratio	R_a, –	0.3818
Flue gas stream ratio	γ_G, –	0.6304
Membrane surface	A_M, m^2	27,100
LHX surface	A_{LHX}, m^2	53,500
HHX surface	A_{HHX}, m^2	86,900
RHX surface	A_{RHX}, m^2	32,300
Total membrane reactor surface	A_{MR}, m^2	199,800

- High heat losses in the flue gas leaving the membrane reactor.
- The need to compress a larger stream of air than the oxygen-depleted air stream expanded in the turbine, which was a consequence of some of the oxygen losses in the ITM. In a classic gas turbine, the expanded stream is higher than the compressed air by the stream of fuel provided in the combustion chamber.
- High-pressure losses of air in the membrane reactor.

The low flue gas temperature at the HRSG inlet (t_{4a}) allowed for the use of steam temperature of 519°C. This was significantly lower value than currently achieved, of up to 600°C, resulting in a lower efficiency of steam cycle η_{elSC} than in modern combined cycle power plants.

The net efficiency of electricity generation η_{el} is the most important indicator allowing for the assessment of a power plant. The largest own needs, at the level of 11.4 MW, were generated by the carbon conditioning unit CCU. In the membrane reactor the electric energy consumed by the circulation fan N_{elCF} was lower than the power generated by the gas-steam turbine N_{elGST}, resulting in a negative total own needs, equal to ΔN_{MR} = –3.6 MW. Thus, the membrane reactor was an additional source of energy in AZEP plant. Finally, the net electric efficiency of AZEP plant η_{el} was at the level of 51.2%, which was the competitive value compared with other concepts of the power plant with oxy-combustion [27,28,38].

6. The influence of membrane parameters on the power plant

The paper presents results of the analyzes of the impact of the improvement of selected properties of the ITM on the parameters of the AZEP plant. The first parameter to be changed was the maximum working temperature of the membrane, while the second was the ion conductivity of the membrane σ_i. For the analyzes all other assumptions were constant, that is, the temperature differences on the HHX hot end and on the RHX cold end, and equaled to $\Delta T_{HE.HHX}$ = 20 K and $\Delta T_{CE.RHX}$ = 40 K, respectively. In order to maintain a constant temperature difference $\Delta T_{HE.HHX}$ and an oxygen content in the flue gas equal to $[O_2]_{1g}$ = 2%, the values of flue gas ratio γ_G and oxygen recovery ratio R_a were changed as the membrane properties change.

6.1. Membrane ion conductivity

The ion conductivity σ_i is a characteristic feature of the material used to make the membrane and, therefore, the change in σ_i value is tantamount to a change of the used material. Thus, the analysis of the change in ion conductivity aimed at providing answers what changes in the AZEP plants performance could be achieved by the development of membranes based on materials with higher oxygen ion permeation intensity than the best currently available materials, such as BSCFO [22]. Because the ion conductivity is not a constant parameter, but changes with the temperature of the membrane according to Eq. (6), the change of σ_i was performed by changing the value of coefficient C_2 in the range from the base value of 517,236 to 1,000,000. The value of σ_i as a function of the membrane temperature t_M for selected values of C_2 is shown in Fig. 2.

The influence of changes in the membrane ion conductivity (through the change of coefficient C_2), on the net efficiency of electricity generation η_{el} of AZEP plant and surfaces of heat exchangers and the membrane in the membrane reactor is shown in Fig. 3.

The improvement of ion conductivity of the membrane M reduced its surface A_M, which led to an increase in the temperature differences in the heat exchangers, also reducing their surface area. The increase in the flue gas temperature at the LHX cold end corresponded to a slight reduction in fuel consumption and corresponding increase in the gas turbine efficiency η_{elGT}. However, at the same time, the change of C_2 from 517,236 (base value) to 1,000,000 has increased the circulation fan's power N_{elCF} by 2.4 MW, that is, by 12%. As a result, the change of C_2 from base value to 1,000,000 allowed for reducing the membrane reactor area A_{MR} by 29%, while the net efficiency of AZEP plant η_{el} decreased by 0.2% point.

Considering the fact that the highest net efficiency of AZEP plant was obtained for such operating parameters, where it was necessary to use very large areas of membrane reactor A_{MR}, the selection of optimal operating parameters of AZEP plant was limited by the maximum surface A_{MR}, in this work adopted at the level of 200,000 m^2. The pressure ratio β = 20 and the flue gas pressure in MR of p_{1g} = 1,800 kPa,

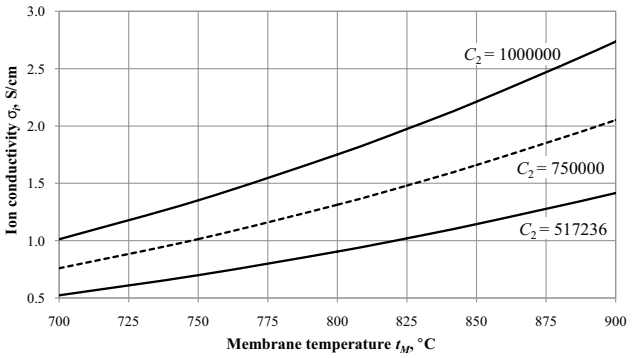

Fig. 2. Ion conductivity of the membrane σ_i as a function of the membrane temperature t_M for selected values of coefficient C_2.

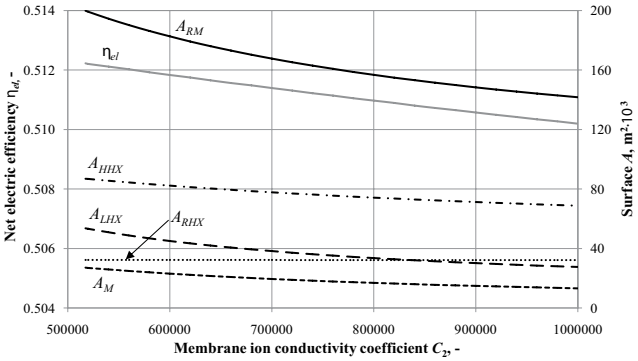

Fig. 3. Net electric efficiency of AZEP plant η_{el} and surfaces A of membrane reactor components as a function of membrane ion conductivity coefficient C_2.

applied in the analysis, were chosen as optimal for the value of coefficient C_2 = 517,236. Therefore, new values of β and p_{1g} were selected for changed value of C_2 to 1,000,000. The analysis was performed for the change of pressure ratio β in a range from 10 to 30, choosing for each β such flue gas pressure p_{1g}, where the membrane reactor area was equal to the maximum A_{MR} = 200,000 m^2, or slightly lower, with step of 10 kPa. In addition, a limitation of the maximum flue gas pressure of $p_{1g} \leq$ 4,000 kPa was assumed in analysis. Results of the analysis are shown in Fig. 4.

The maximum net efficiency of AZEP plant η_{el} = 0.5173 was obtained for β = 17 and p_{1g} = 2,150 kPa, which meant that the improvement of the ion conductivity of the membrane by approximately 93% allowed to raise the net efficiency of the power plant by 0.51% point.

6.2. Maximum membrane temperature

The maximum working temperature of the membrane is primarily related to its high-temperature resistance. The maximum temperature of 900°C, adopted in the analysis, was a limitation not resulting from the resistance of dense layer of the membrane, but a porous support used to ensure sufficient mechanical resistance to high-pressure differences on both sides of the membrane. The porous support is usually made of the same material as the dense layer, but shaped at

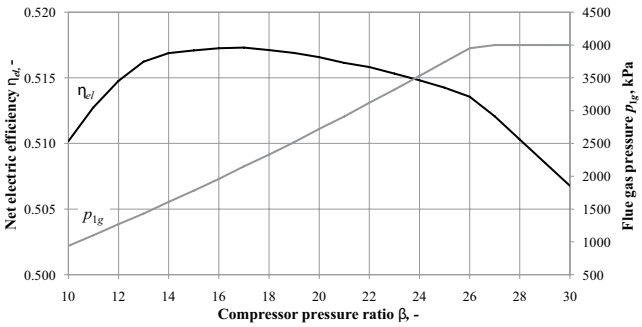

Fig. 4. Net electric efficiency of AZEP plant η_{el} and flue gas pressure p_{1g} as a function of compressor pressure ratio β for coefficient C_2 = 1,000,000.

temperature of 1,050–1,100°C to avoid its sintering. It means, that the long-term exposure of the porous support to high temperatures of 1,000–1,050°C causes its sintering, reducing its permeability and, thus, reducing the ion conductivity of the entire membrane.

The increase of the membrane operating temperature should allow to improve its operating parameters, since, according to Eq. (6), the ion conductivity σ_i is significantly dependent on the membrane temperature T_M. The highest temperature observed in the membrane was the flue gas temperature at the membrane hot end t_{3g}, therefore, the analysis of the influence of changing t_{3g} in a range from base value of 900°C to 1,050°C on the parameters of the AZEP plant, was performed. The change of ion conductivity σ_i as a function of membrane temperature t_M, for the base value of coefficient C_2 = 517,236, is shown in Fig. 5. The influence of flue gas temperature t_{3g} on the net efficiency of the AZEP plant η_{el} and the surfaces of the membrane and the heat exchangers in the membrane reactor are shown in Fig. 6.

The increase in flue gas temperature t_{3g}, analogous to the membrane ion conductivity increase, reduced the membrane surface A_M, which led to an increase in temperature differences in the heat exchangers, also reducing their surface areas. The fuel consumption reduction resulting from the LHX cold end flue gas temperature raise, corresponded to an increase in the gas turbine efficiency, but with slight decreases in the electric power of steam turbine ST and gas-steam turbine GST, at the same time. The LHX hot end flue gas temperature raise in combination with the increase

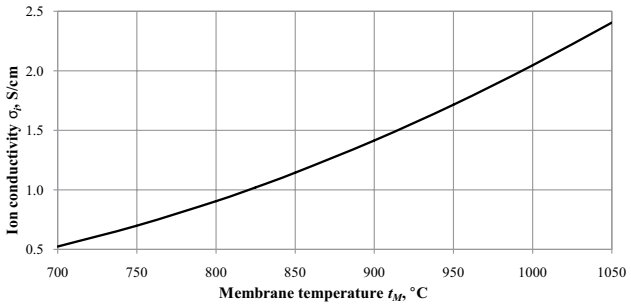

Fig. 5. Membrane ion conductivity σ_i as a function of the membrane temperature t_M for the value of coefficient C_2 = 517,236.

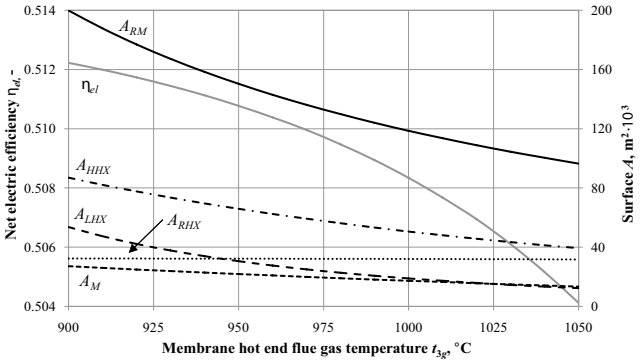

Fig. 6. Net electric efficiency of AZEP plant η_{el} and surfaces A of membrane reactor components as a function of membrane hot end flue gas temperature t_{3g}.

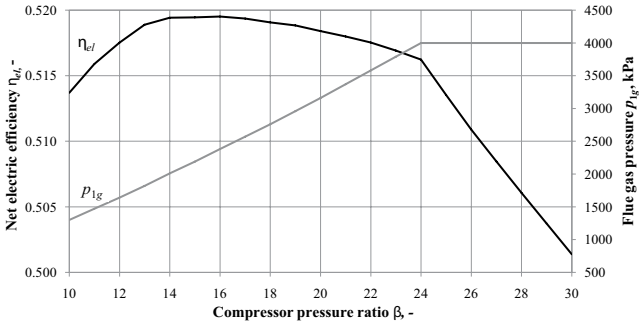

Fig. 7. Net electric efficiency of AZEP plant η_{el} and flue gas pressure p_{1g} as a function of compressor pressure ratio β for flue gas temperature t_{3g} = 1,050°C.

of its flux with the change of t_{3g} from 900°C to 1,050°C, increased the electric power of circulation fan by 10 MW, that is, by 50%.

The total efficiency drop by 0.81% point with a temperature raise from 900°C to 1,050°C was primarily caused by the growth of the circulation fan own needs. However, a significant reduction in the membrane reactor area A_{RM} by 51.5% was obtained. Therefore, in analogy to the previous analysis, new values of β and p_{1g} were selected with the conditions of the maximum membrane reactor area $(A_{RM})_{max}$ = 200,000 m^2 and maximum flue gas pressure $(p_{1g})_{max}$ = 4,000 kPa. The results of the analysis are shown in Fig. 7.

The maximum net efficiency of AZEP plant η_{el} = 0.5195 was obtained for β = 16 and p_{1g} = 2,380 kPa, which meant, that increasing the maximum flue gas temperature in the membrane from 900°C to 1,050°C improved the net power plants efficiency by 0.73% points.

Table 2
Selected characteristic parameters of the AZEP plant cases: AZEP, AZEP_1, and AZEP_2

Parameter	Symbol, unit	AZEP	AZEP_1	AZEP_2
Fuel chemical energy flux	$\dot{m}_f LHV$, MW	571.0	588.6	595.4
Gas turbine electric power	N_{elGT}, MW	200.0	200.0	200.0
Turbine internal power	N_{iT}, MW	497.6	473.9	465.8
Compressor internal power	N_{iC}, MW	290.6	267.1	259.1
Gas turbine electric efficiency	η_{elGT}, –	0.3502	0.3398	0.3359
Gas turbine outlet air heat flow	$\dot{Q}_{4a}$, MW	336.1	354.6	362.3
Steam turbine electric power	N_{elST}, MW	106.4	117.4	121.9
Steam cycle electric efficiency	η_{elSC}, –	0.3144	0.3288	0,3341
Power plant gross electric power	$N_{el.gross}$, MW	306.4	317.4	321.9
Power plant gross electric efficiency	$\eta_{el.gross}$, –	0.5366	0.5393	0.5407
Gas turbine and steam cycle own needs	ΔN_{CC}, MW	6.1	6.8	6.9
Gas-steam turbine electric power	N_{elGST}, MW	23.6	24.4	24.8
Circulation fan electric power	N_{elCF}, MW	20.0	19.2	19.1
Membrane reactor own needs	ΔN_{MR}, MW	–3.6	–5.2	–5.7
CO_2 conditioning unit own needs	ΔN_{CCU}, MW	11.4	11.3	11.4
Total power plant own needs	ΔN_{el}, MW	13.9	13.0	12.6
Total power plant own needs ratio	δ_{el}, –	0.0454	0.0408	0.0391
Power plant net electric power	N_{el}, MW	292.5	304.5	309.3
Power plant net electrical efficiency	η_{el}, –	0.5122	0.5173	0.5195
Oxygen recovery ratio	R_a, –	0.382	0.396	0.401
Flue gas stream ratio	γ_G, –	0.630	0.631	0.633
Membrane surface	A_M, m^2	27,100	25,500	52,500
LHX surface	A_{LHX}, m^2	53,500	55,900	53,000
HHX surface	A_{HHX}, m^2	86,900	84,200	57,600
RHX surface	A_{RHX}, m^2	32,300	34,400	34,900
Total membrane reactor surface	A_{MR}, m^2	199,800	200,000	198,000

Table 2 presents selected operating parameters of three cases of the AZEP plant:

- base case AZEP (C_2 = 517,236, t_{3g} = 900°C, β = 20, p_{1g} = 1,800 kPa),
- case AZEP_1 (C_2 = 1,000,000, t_{3g} = 900°C, β = 17, p_{1g} = 2,150 kPa),
- case AZEP_2 (C_2 = 517,236, t_{3g} = 1,050°C, β = 16, p_{1g} = 2,380 kPa).

7. Summary

The paper presents the model of zero-emission combined cycle power plant integrated with membrane reactor AZEP, which uses ITM, and analyzes of the impact of key membrane properties on the operating parameters of the power plant. The analysis of the base power plant indicated that with currently available membranes and other limitations of AZEP plant (e.g. high-pressure losses and low admissible temperatures in the membrane reactor) it was possible to achieve the net efficiency of electricity generation η_{el} at the level of 0.512, which was competitive with other concepts of zero-emission combined cycle power plants.

Performed analyzes showed that while maintaining constant pressure levels in the gas turbine (β) and in the membrane reactor (p_{1g}), the improvement of both membrane properties associated with increasing oxygen diffusion intensity through the membrane (i.e., membrane ion conductivity coefficient C_2 and membrane hot end flue gas temperature t_{3g}) allowed for the reduction of the surfaces of membrane A_M and the entire membrane reactor A_{RM}, but at the loss of the net electricity generation efficiency of AZEP plants η_{el} (Figs. 3 and 6). However, the choice of new β and p_{1g} values for the assumed improvement of C_2 in case AZEP_1, and t_{3g} in case AZEP_2, respectively, with the maximum membrane reactor area of $(A_{RM})_{max}$ = 200,000 m², allowed to improve the net electric efficiency η_{el} by 0.51% and 0.73% points, respectively, compared with the base AZEP plant. The net efficiency increase was obtained by both, the increase of the gross electric efficiency $\eta_{el.gross}$, as well as the reduction of the own needs of the membrane reactor ΔN_{MR}.

Analyzes showed, that the development and the use of ITM with higher ion conductivity σ_i or with higher maximum operating temperature t_M in AZEP power plants would allow to reduce the membrane reactor area A_{MR}, or to improve the efficiency of the power plant, while maintaining the same A_{MR}. Thus, the development of ITM for potential application in AZEP plants would allow to reduce fuel consumption and reduce the size of membrane reactor and related investment costs.

Acknowledgments

The article was written within statutory research funds of Silesian University of Technology.

Symbols

A — Surface area, m²
C — Constant coefficient, –
d — Membrane thickness, m
E_a — Activation energy for ion conductivity, kJ/mol
F — Faraday's constant, $F \approx 9.6485 \times 10^4$ C/mol
j_{O_2} — Unit flow of oxygen ions permeated through membrane, mol/(m² s)
k — Heat transfer coefficient, W/(m² K)
LHV — Lower heating value, MJ/kg
M — Specific molar mass, kg/kmol
n — Number of carrier charges, number of membrane parts in membrane model, –
N — Power, MW
p — Pressure, kPa
p_{O_2} — Partial oxygen pressure, kPa
$\dot{Q}$ — Heat flux, MW
R — Universal gas constant, $R \approx 8.3145$ J/(mol K)
R_a — Membrane oxygen recovery ratio, –
t, T — Temperature, °C, K

Greek symbols

β — Compression rate, –
γ_G — Flue gas stream ratio, –
δ_{el} — Own needs rate of power plant, –
ΔT — Temperature difference, K
ΔN — Auxiliary power, MW
ζ — Pressure loss rate, –
η — Efficiency, –
σ_i — Membrane ion conductivity, S/m

Indexes

a, *A* — Air
el — Electric
g, *G* — Flue gas
i — Isentropic, number of actual membrane part in iterative calculations
m — Mechanical
max — Maximum
min — Minimum
s — Steam or water in steam cycle

References

[1] Climate Change 2014: Synthesis Report, Intergovernmental Panel on Climate Change, Geneva, Switzerland, 2015.
[2] Energy and Climate Change, World Energy Outlook Special Report, International Energy Agency, 2015.
[3] K. Badyda, A. Miller, Energetyczne turbiny gazowe oraz układy z ich wykorzystaniem, Kaprint, Lublin, 2014. [in Polish]
[4] T. Chmielniak, A. Rusin, K. Czwiertnia, Turbiny gazowe, Ossolineum, Wrocław, 2001. [in Polish]
[5] J. Kotowicz, Elektrownie gazowo-parowe, Kaprint, Lublin, 2008. [in Polish]
[6] E. Yantovsky, J. Górski, M. Shokotov, Zero Emissions Power Cycles, CRC Press, Boca Raton, FL, 2009.
[7] L. Zheng, Oxy-fuel combustion for power generation and carbon dioxide (CO_2) capture, Woodhead Publishing Limited, Cambridge, UK, 2011.
[8] J. Tranier, R. Dubettier, A. Darde, N. Perrin, Air Separation, flue gas compression and purification units for oxy-coal combustion systems, Energy Procedia, 4 (2011) 966–971.
[9] A. Skorek-Osikowska, Ł. Bartela, J. Kotowicz, M. Job, Thermodynamic and economic analysis of the different variants of a coal-fired, 460MW power plant using oxy-combustion technology, Energy Convers. Manage., 76 (2013) 109–120.

[10] M. Job, Ł. Bartela, A. Skorek-Osikowska, Analysis of the use of waste heat in an oxy-combustion power plant to replace steam cycle heat regeneration, J. Power Technol., 93 (2013) 133–141.
[11] A.R. Smith, J. Klosek, A review of air separation technologies and their integration with energy conversion process, Fuel Process. Technol., 70 (2001) 115–134.
[12] J. Kotowicz, A. Balicki, Enhancing the overall efficiency of a lignite-fired oxyfuel power plant with CFB boiler and membrane-based air separation unit, Energy Convers. Manage., 80 (2014) 20–31.
[13] J. Kotowicz, S. Michalski, Efficiency analysis of a hard-coal-fired supercritical power plant with a four-end high-temperature membrane for air separation, Energy, 64 (2014) 109–119.
[14] K. Janusz-Szymańska, O. Dryjańska, Possibilities for improving the thermodynamic and economic characteristics of an oxy-type power plant with a cryogenic air separation unit, Energy, 85 (2015) 45–61.
[15] S. Berdowska, A. Skorek-Osikowska, Technology of oxygen production in the membrane-cryogenic air separation system for a 600 MW oxy-type pulverized bed boiler, Arch. Thermodyn., 33 (2012) 65–76.
[16] S.M. Hashim, A.R. Mohamed, S. Bhatia, Current status of ceramic-based membranes for oxygen separation from air, Adv. Colloid Interface Sci., 160 (2010) 88–100.
[17] M.A. Habib, M.A. Nemitallah, Design of an ion transport membrane reactor for application in fire tube boilers, Energy, 81 (2015) 787–801.
[18] J. Sunarso, S. Baumann, J.M. Serra, W.A. Meulenberg, S. Liu, Y.S. Lin, J.C. Diniz da Costa, Mixed ionic–electronic conducting (MIEC) ceramic-based membranes for oxygen separation, J. Membr. Sci., 320 (2008) 13–41.
[19] M.D. Mancini, A. Mitsos, Ion transport membrane reactors for oxy-combustion - part I: intermediate-fidelity modeling, Energy, 36 (2011) 4701–4720.
[20] F. Selimovic, Computational Analysis and Modeling Techniques for Monolithic Membrane Reactors Related to CO_2 Free Power Processes, Doctoral Thesis, Lund University, Lund, Sweden, 2007.
[21] K. Foy, J. McGovern, Comparison of Ion Transport Membranes, Proceedings of Fourth Annual Conference on Carbon Capture and Sequestration DOE/NETL, Alexandria, USA, 2005.
[22] H. Lu, Y. Cong, W.S. Yang, Oxygen permeability and stability of Ba0.5 Sr0.5 Co0.8 Fe0.2 O3-d as an oxygen-permeable membrane at high pressures, Solid State Ionics, 177 (2006) 595–600.
[23] M.A. Nemitallah, M.A. Habib, K. Megzhani, Experimental and numerical study of oxygen separation and oxy-combustion characteristics inside a button-cell LNO-ITM reactor, Energy, 84 (2015) 600–611.
[24] S. Baumann, J.M. Serra, M.P. Lobera, S. Escolástico, F. Schulze-Küppers, W.A. Meulenbenrg, Ultrahigh oxygen permeation flux through supported $Ba_{0.5}Sr_{0.5}Co_{0.8}Fe_{0.2}O_{3-\delta}$ membranes, J. Membr. Sci., 377 (2011) 198–205.
[25] S.G. Sundkvist, S. Julsrud, B. Vigeland, T. Naas, M. Budd, H. Leistner, D. Winkler, Development and testing of AZEP reactor components, Int. J. Greenhouse Gas Control, 1 (2007) 180–187.
[26] B.F. Möller, T. Torisson, M. Assadi, AZEP Gas Turbine Combined Cycle Power Plants - Thermo-economic Analysis, Intern. J. Thermodyn., 9 (2006) 21–28.
[27] H.M. Kvamsdal, K. Jordal, O. Bolland, A quantitive comparison of gas turbine cycles with CO_2 capture, Energy, 32 (2007) 10–24.
[28] F. Petrakopoulou, G. Tsatsaronis, A. Boyano, T. Morosuk, Exergoeconomic and exergoenvironmental evaluation of power plants including CO_2 capture, Chem. Eng. Res. Design, 89 (2011) 1461–1469.
[29] M.A. Habib, P. Ahmed, R. Ben-Mansour, H.M. Badr, P. Kirchen, A.F. Ghoniem, Modeling of a combined ion transport and porous membrane reactor for oxy-combustion, J. Membr. Sci., 446 (2013) 230–243.
[30] S. Gunasekaran, N.D. Mancini, A. Mitsos, Optimal design and operation of membrane-based oxy-combustion power plants, Energy, 70 (2014) 338–354.
[31] Gate Cycle Version 5.40. Manual, GE Enter Software, LLC.
[32] J. Kotowicz, M. Job, M. Brzęczek, The characteristics of ultramodern combined cycle power plants, Energy, 92 (2015) 197–211.
[33] J. Kotowicz, M. Brzęczek, M. Job, The influence of carbon capture and compression unit on the characteristics of ultramodern combined cycle power plant, Int. J. Global Warming, 12 (2017) 164–187.
[34] J. Kotowicz, Ł. Bartela, The influence of economic parameters on the optimal values of the design variables of a combined cycle plant, Energy, 35 (2010) 911–919.
[35] E. Yantovsky, J. Górski, B. Smyth, J. ten Elshof, Zero-emission fuel-fired power plants with ion transport membrane, Energy, 29 (2004) 2077–2088.
[36] J. Kotowicz, M. Job, Modeling a membrane reactor for a zero-emission combined cycle power plant, J. Power Technol., 97 (2017) 7–14.
[37] M. Job, Modelowanie i analiza zaawansowanych technologicznie zeroemisyjnych elektrowni gazowo-parowych ze spalaniem tlenowym, Politechnika Śląska, Gliwice, 2017. [in Polish]
[38] J. Kotowicz, M. Job, Porównanie termodynamiczne zeroemisyjnych elektrowni gazowo - parowych ze spalaniem tlenowym, Rynek Energii, 6 (2016) 36–42. [in Polish]